Modeling the Swelling Curve for Packed Soil Aggregates Using the Pedostructure Concept

Erik Braudeau* and Rabi H. Mohtar

ABSTRACT

The swelling curve is generally studied as structural soil volume dependence on water content during swelling, and not on time. In this paper, we show how the swelling curve defined as the specific volume of the soil as a function of time, $V(t)$, represent the dynamic properties of the pedostructure where the shrinkage curve represents and characterizes the hierarchical and functional organization of the soil medium. This paper presents the development and experimental evaluation of the swelling curve for a dry bed of packed aggregates immersed in water using the pedostructure concept. Pedostructure-based parametric functions for the soil structure and water interaction represented by soil shrinkage and matric water potential curves were used to derive the swelling curve equation. This equation represents the kinetic of absorption of water by swelling of the primary peds within the pedostructure. Experiments on wetting-drying cycles of reconstituted soil samples were conducted to obtain the parameters needed for the swelling curve equation. The simulated swelling curves using the derived equation agreed well with the measured data. The new swelling equation shows only one additional parameter; namely, the time to half charge, $t^{1/2}$, which seems to be a characteristic of the clay type. It was found to be near 2100 s for kaolinitic soils and found to be independent of the clay content; as it decreased by a factor of two to three due to the presence of smectites in the sample. This paper gives access to the study of the kinetic of water absorption by primary peds.

Soil swelling curves in soil science literature are typically associated with saturated state. Most authors associate the swelling curve to its shrinking counterpart and refer to it as the Shrinkage-Swelling Characteristic or SSC (Bronswijk, 1988; Kim et al., 1992; Kim et al., 1999). Thus, the swelling curve is usually understood as soil volume dependence on water content during swelling, but not as a time dependent equation. However, in the present paper we will consider the swelling curve as a time dependent soil volume change during swelling. In fact, most soil swelling properties are examined from soil dynamics point of view for highly swelling soils (Rollins et al., 1961; Favre et al., 1997; Michel et al., 2000; Greco, 2002; Chertkov, 2004). These studies are usually triggered by soil management issues such as the need to reduce soil damage or improve field trafficability (Sarmah et al., 1996; Kirby and Ringrose-Voase, 2000; Horn et al., 2003) or to account for water bypass and preferential flow problems caused by soil cracking (Hammel et al., 1999; Greco, 2002; Van Dam, 2000; Logsdon, 2002; Wells et al., 2003; Braudeau et al., 2004a). Only few studies (Ruy et al., 1999; Chertkov, 2004; Braudeau et al., 2004b) took account of the internal organization of the soil fabric in their model. As a consequence, no relationship between the dynamics of the soil organization and absorption of the water by the clayey plasma within the soil fabric is yet known.

Therefore, the swelling curve (S_wC), the structured soil specific volume (V) as a function of time (t) during swelling and the complementary part of the shrinking curve in the wetting-drying cycles of soils, merits consideration. Under laboratory conditions, the shrinkage curve [$V(W)$, V as a function of water content, W, in the drying cycle] was considered by Braudeau et al. (2004b) as a succession of equilibrium states $(W, V)^{eq}$ of which the hydrostructural configuration is fully determined. They showed that the S_hC is the soil moisture characteristic curve, which defines the functional specific volumes of the soil fabric such as primary peds, interpedal porosity, macropore water content, etc. Following this point of view, the S_wC, describes the water sorption rate by primary peds and can be used to define the kinetics of the medium at a given (V, W) configuration on its way to the equilibrium as defined by the S_hC. We believe that it is this property of the swelling curve that needs to be studied; and consequently, this article would be a contribution to this aspect of the S_wC.

The objective of this paper is to develop and evaluate an equation for the swelling curve for a bed of packed aggregates using the pedostructure concept. Swelling and shrinking cycles of reconstituted soil samples (packed <2-mm sieved aggregates), will be examined. Two basic hypotheses were used in this study:

Water absorption by the primary peds is due to the hydration forces in water layers at the surface of the clay particles inside the primary peds (swelling pressure, Ps_{mi}), in accordance to the scheme proposed by Braudeau and Mohtar (2004) for the macropore water potential (the tensiometric curve h_{ma}).

The organizational parameters of the soil sample determined using the S_hC are constant in the swelling-drying cycles. Thus, parameters and variables that are defined by the S_hC measured during the drying stage can be used during the swelling part of the cycle.

THEORY

Soil Medium Organizational Variables and Parameters According to the S_hC

Figure 1 shows a schematic representation of the soil fabric with its three hierarchical functional levels; namely, the pedostruture, the primary peds and the

E. Braudeau, Institut de Recherche pour le Développement (IRD), Pôle de Recherche Agronomique de la Martinique, BP 214, F-97283 Le Lamentin, Martinique, France; R.H. Mohtar, Agric. and Biological Engineering, Purdue Univ., West Lafayette, IN 47906, USA. Received 28 June 2004. *Corresponding author (erik.braudeau@ird.fr).

Published in Soil Sci. Soc. Am. J. 70:494–502 (2006).
Soil Physics
doi:10.2136/sssaj2004.0211

677 S. Segoe Rd., Madison, WI 53711 USA

Abbreviations: S_hC, shrinkage curve; S_wC, swelling curve.

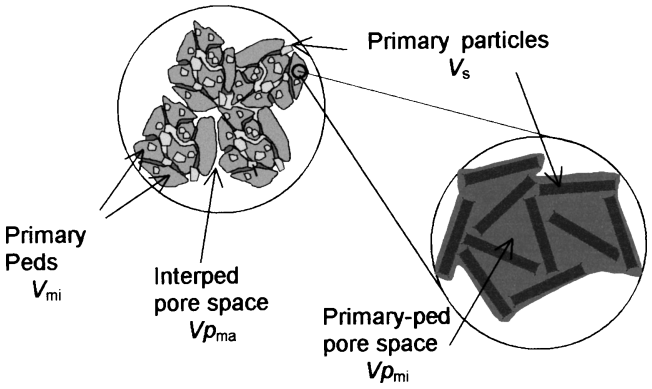

Fig. 1. Schematic representation of the pedostruture composed of primary peds and primary particles.

primary particles (Braudeau et al., 2004b). The pedostructure includes the primary peds (V_{mi}) and the pore space created by their assembly (Vp_{ma}). The specific pore volume of primary peds (Vp_{mi}) is quantitatively defined by the water content at the air entry point (W_B), which is identified as point B on a continuously measured shrinkage curve (Fig. 2). Indeed, at this point, the following equation holds: $Vp_{mi} = W_B/\rho_w$. The water content in the primary peds and the interped macropore space are written W_{mi} and W_{ma}, respectively. The interped macropore water pool consists of two types of water, w_{ip} and w_{st}, that are differentiated and defined according to the linear shrinkage phases, the interped and the structural shrinkage phase, respectively (Braudeau et al., 2004b), such as $W_{ma} = w_{ip} + w_{st}$. These types of water are defined as swelling water, w_{ip}, water that leaves interped pores without air entry (peds are approaching each other) and nonswelling water, w_{st}, water that leaves the same pore system while being replaced by air (peds are jointed). The later is associated with weak or no shrinkage of the interped pore system. At the micro pore scale, the primary peds are composed of the primary particles (clay, silt, and sand) of specific volume V_s, and of the micropore space between them. In this micropore space, two types of water are also defined according to the corresponding basic and residual linear shrinkage phases, namely: a swelling water, w_{bs}, and a nonswelling water, w_{re}. The subscripts *ip*, *st*, *bs*, and *re* were given by Braudeau et al. (2004b) according to the classical nomenclature of the linear shrinkage phase from which each type of water was defined, namely: interped, structural, basic and residual shrinkage phase. All these organizational pedostructure variables (specific volumes, waters contents, specific pore volumes) are summarized in Table 1. All variables are in reference to the mass of primary particles that are present in the soil volume under consideration.

According to their interpretation of the structural soil volume dependence on water content and using observed data to validate their equation, Braudeau et al. (2004b) introduced the following shrinkage curve:

$$dV = K_{re}dw_{re} + K_{bs}dw_{bs} + K_{st}dw_{st} + K_{ip}dw_{ip} \quad [1]$$

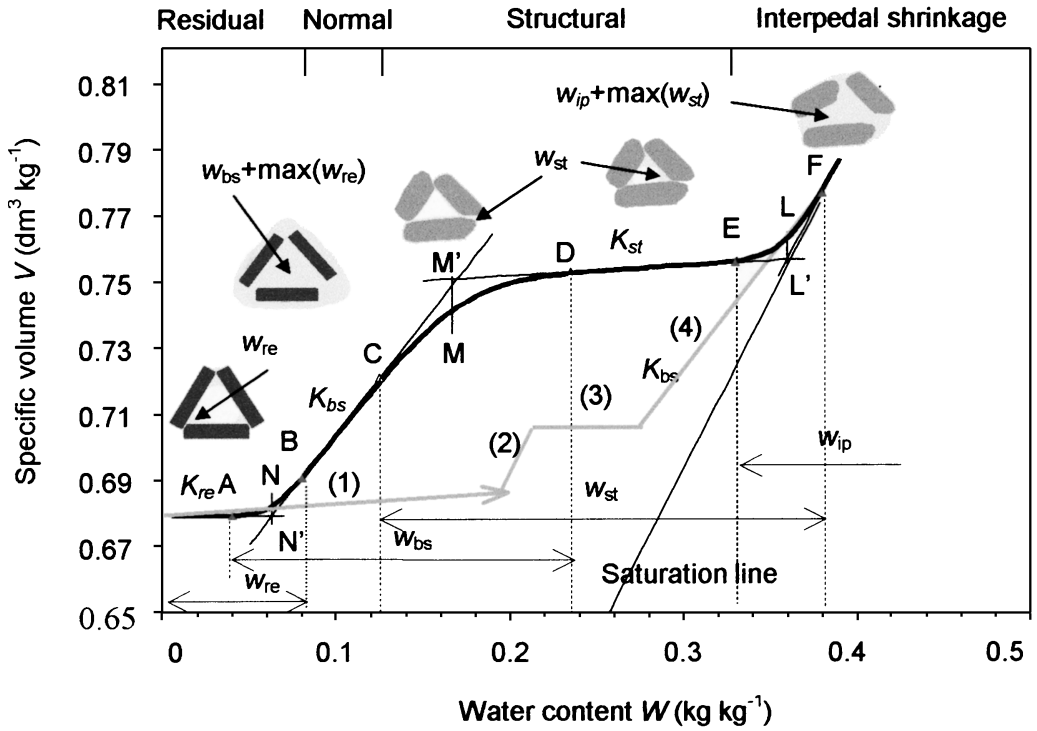

Fig. 2. Various configurations of air and water partitioning into the two pore systems, inter and intra primary peds, related to the shrinkage phases of a standard Shrinkage Curve. The polygon lines (1), (2), …, represent the assumed swelling path steps of a bed of packed soil aggregates which is smoothly immersed in the water under conditions described in the article. The various water pools, w_{re}, w_{bs}, w_{st}, w_{ip}, are represented with their domain of variation. The linear and curvilinear shrinkage phases are delimited by the transition points (A, B, C, D, E, and F). Points N′, M′, and L′ are the intersection points of the tangents at those linear phases of the SC.

Table 1. Summary of hydrostructural variables for the unsaturated soil-water medium at the pedostructure and horizon scales, respectively.

Volume of concern	Specific volume	Specific pore volume	Water content	Non swelling water	Swelling water	Suction pressure
Pedostructure	V		W			h
Interpedal porosity		Vp_{ma}	W_{ma}	w_{st}	w_{ip}	h_{ma}
Primary peds	V_{mi}	Vp_{mi}	W_{mi}	w_{re}	w_{bs}	h_{mi}
Primary soil particles	V_s					

where $K_{(s)}$ are the slopes of the linear shrinkage phases (Fig. 2) and they represent the pedostructure volume change caused by the change of the various water pools. The slopes are considered as structural parameters of the pedostructure, linking the macroscopic assembly level to the water pools levels. As an example:

$$K_{bs} = \partial V/\partial w_{bs} = (1/\rho_w)\partial V/\partial V\rho_{mi} = (1/\rho_w)\partial V/\partial V\rho_{mi} \quad [2]$$

where ρ_w is the water density in kg dm^{-3}. Using Eq. [1] and the definitions of the pedostructure variables and parameters, all the descriptive variables of the soil organization listed in Table 1 can be formulated as a function of the water contents in the various pools. This is the reason that the S_hC is needed to determine the structural parameters and variables relationships that are required for modeling the pedostructure swelling in the wetting-drying cycle.

That is the case for the parameters W_N, W_M, W_L of the shrinkage curve, which are, respectively, the water contents at the intersection points N′, M′, L′ of the tangent lines extending the quasi-linear shrinkage regions of the shrinkage curve (Fig. 2). These parameters are easily determined from the shrinkage curve and represent three major characteristics of the two pore systems according to the following relationships:

$$W_N/\rho_w = \max(w_{re})/\rho_w = \min(Vp_{mi}) \quad [3]$$

$$W_M/\rho_w = [\max(w_{re}) + \max(w_{bs})]/\rho_w = \max(Vp_{mi}) \quad [4]$$

$$(W_L - W_M)/\rho_w = \max(w_{st})/\rho_w = Vp_{ma} \quad [5]$$

where $\max(w_{re})$ and $\max(w_{bs})$ are the maximum values of w_{re} and w_{bs} that correspond to $W = W_B$ and $W = W_D$, respectively (see Fig. 2).

Interaction of Water with the Soil Fabric

Braudeau and Mohtar (2004) showed that the typical tensiometric curve, that is, the soil moisture characteristic curve measured using a tensiometer, depends solely on the interpedal water content, W_{ma}. This tensiometric pressure was defined as h_{ma} and refers to the suction of water in the macropore space. The authors developed equations and parameters for h_{ma} in accordance to the thermodynamic theory of Voronin (1980), Berezin et al. (1983) and Low (1987), which considers water in the soil fabric as a film surrounding particles and aggregates. Proceeding from the osmotic theory of the interaction of a charged surface in contact with water, Voronin (1980) defined the swelling pressure, P_s, (in kPa) as:

$$P_s = \frac{\rho_w Q_s RT}{W - W_\sigma} = \frac{E\rho_w}{W - W_\sigma} \quad [6]$$

where $E = Q_s\,RT$, is the potential energy of the solid phase resulting from the surface charge of the soil, in J kg^{-1} of solids; Q_s is the effective electric charge of the surface or effective exchange capacity in mol kg^{-1} of solids; R is the molar gas constant in J mol^{-1}K^{-1} and T the absolute temperature; W_σ is the quantity of stable-bound water that does not contribute to the creation of the diffuse layer and corresponds to the state of a completely formed wetting water film.

Adapting Eq. [6] to the micro-organization of the pedostructure, the swelling pressure of the water layer in primary peds, Ps_{mi}, can be written as:

$$Ps_{mi} = \rho_w E_{mi}/[W_{mi} - \max(w_{re})] = \rho_w E_{mi}/w_{bs} \quad [7]$$

where E_{mi} is the potential energy of the solid phase (per unit mass of solids) resulting from the surface charge of the primary particles into the primary peds; and the Voronin term W_σ is identified with $\max(w_{re})$ that does not participate in any swelling.

Hydrostructural Dynamic of the Pedostructure

The basic assumption for the development of the pedostructure functional model is that all of the hydrostructural equilibrium configurations are defined by the shrinkage curve (S_hC) under laboratory conditions; the changes in internal organization of the pedostructure during the drying cycle as a result of evaporation is slow enough that all points of the S_hC can be considered at thermodynamic equilibrium. Equilibrium configuration here is represented by point $(W, V)^{eq}$ on the S_hC which corresponds to single values of w_{re}, w_{bs}, w_{st}, and w_{ip}, and thus, of all the other organizational variables of the pedostructure of Table 1.

The dynamics of the soil water pools and the pedostructure can be studied by setting the pedostructure at point (W, V) outside the S_hC and measuring the volume change over time (V, t) during the return to the equilibrium state at (W, V^{eq}). Nonequilibrium states occur naturally when water is added to the interped macroporosity ($w_{st} > w_{st}^{eq}$) or when the interped water is rapidly extracted ($w_{st} < w_{st}^{eq}$). The resulting pedostructure volume change over time will be swelling in the first case and shrinking in the second. These two dynamics, swelling and shrinking, can be assumed to be governed by the same conceptual process of water exchange between the primary peds and the interped pore space. If we assume that Pc is the cohesive pressure of the assembly which acts like an envelope pressure for the primary peds such that, at equilibrium (Fig. 3),

$$Ps_{mi} = h_{ma} + Pc \quad [8]$$

then the suction pressure inside the primary peds, h_{mi}, can be defined as:

$$h_{mi} = Ps_{mi} - Pc$$

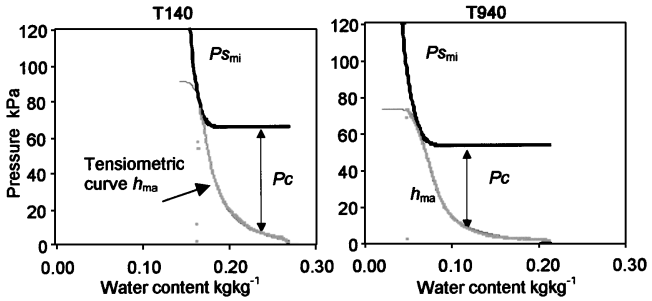

Fig. 3. Graphs representing the water suction in macropore, h_{ma} (gray dots), the swelling pressure in primary peds Ps_{mi} (black line), and the cohesive pressure on the primary peds, Pc. The h_{ma} curves are measured tensiometric curves given in Braudeau and Mohtar (2004) for two soil samples of this study, and the Ps_{mi} curves are modeled according to $Ps_{mi} = \rho_w E_{mi}/w_{bs}$ (Eq. [7]).

with Ps_{mi} and Pc depending, respectively, on w_{bs} and W_{ma}. Then the water exchange between the two media is proportional to the difference in their pressure such as:

$$\frac{dw_{bs}}{dt} = k_{mi}(Ps_{mi} - h_{ma} - Pc) = -\frac{dw_{st}}{dt} \qquad [9]$$

where k_{mi} is a transfer rate coefficient ($kg_{water}\ kg^{-1}_{soil}\ kPa^{-1}s^{-1}$) for the absorption–desorption of water by the primary peds. At equilibrium, we note that $h = h_{mi} = h_{ma}$; however, out of equilibrium, $h_{mi} = Ps_{mi}(w_{bs}) - Pc(W_{ma}) \neq h_{ma}(W_{ma})$. The transfer rate coefficient, k_{mi}, expresses the velocity of the layers of water on the surface of the clay particles within the primary peds. Because this surface is constant, k_{mi} can also be considered constant over a large range of water content, on condition that in this range, the change of viscosity of the added water layer is negligible. This can be justified conceptually by the fact that water enters into the plasma and then successively adds layers of water at the surface of all the particles inside the primary peds.

For an equilibrium configuration, according to Eq. [8]

$$P_c^{eq} = Ps_{mi}^{eq} - h_{ma}^{eq} \qquad [10]$$

In the particular case where the sample is immersed in water, $h_{ma} = 0$ all along the swelling process, and

$$Pc^{sat} = Ps_{mi}{}^{sat} = \rho_w E_{mi}/\max(w_{bs}) = \rho_w E_{mi}/(W_M - W_N) \qquad [11]$$

Applied to this case Eq. [9] can be rewritten as:

$$\frac{dw_{bs}}{dt} = \rho_w k_{mi} E_{mi}\left(\frac{1}{w_{bs}} - \frac{1}{W_M - W_N}\right) \qquad [12]$$

This last equation will be used for modeling the swelling curve.

Modeling the Swelling Curve

Figure 2 shows a schematic representation of the swelling phases relative to the S_hC. This process involves the following stages:

Entry of water into the soil medium through the interped voids;
Enlargement of the interaggregate space;
Entry of water into the dry micropores of the primary peds filling the residual micropore dry space; and
Swelling of the primary peds.

The first three stages occur simultaneously, but are represented separately starting from Point A by three segments marked on Fig. 2 as segments (1), (2), (3) of known x-lengths: $\max(w_{st}) = W_L - W_M$, $w_{ip} = W_F - W_L$ and $\max(w_{re}) = W_N$; and slopes: K_{st}, 1 and 0, respectively, according to the structural relationships above (Eq. [1]–[5]). The swelling of the primary peds is the last event driving the sample along Segment (4) of slope K_{bs} and x-length of $\max(w_{bs}) = W_M - W_N$. In this conceptual swelling path, it is assumed that the structural parameters are stable and did not change during the shrinkage-swelling cycles.

Equation [12] can be written as:

$$\frac{w_{bs}dw_{bs}}{(W_M - W_N) - w_{bs}} = \frac{\rho_w k_{mi} E_{mi}}{(W_M - W_N)}dt \qquad [13]$$

Integration in the swelling Step (4) in Fig. 2, between $(t = 0, w_{bs} = 0)$ and (t, w_{bs}), gives:

$$\mathrm{Log}\left[\frac{(W_M - W_N) - w_{bs}}{W_M - W_N}\right] + \frac{w_{bs}}{W_M - W_N} = -\frac{\rho_w k_{mi} E_{mi}}{(W_M - W_N)^2}t \qquad [14]$$

Taking into account that structural and residual shrinkages are negligible, using Eq. [2] allows us to write the following:

$$(V_{max} - V) = K_{bs}[\max(w_{bs}) - w_{bs}] = K_{bs}(W_M - W_N - w_{bs})$$

where V_{max} is the specific volume of the soil sample at large time values ($t = \infty$), which can be evaluated directly from the swelling curve. Therefore, Eq. [14] becomes:

$$\mathrm{Log}\left[\frac{V_{max} - V}{K_{bs}(W_M - W_N)}\right] + 1 - \frac{V_{max} - V}{K_{bs}(W_M - W_N)} = -\frac{\rho_w k_{mi} E_{mi}}{(W_M - W_N)^2}t \qquad [15]$$

that can be put into the form:

$$\mathrm{Log}\left(\frac{V_{max} - V}{B}\right) + 1 - \frac{V_{max} - V}{B} = -At \qquad [16]$$

where:

$$A = \rho_w k_{mi} E_{mi}/(W_M - W_N)^2 \qquad [17]$$

$$B = K_{bs}(W_M - W_N) \qquad [18]$$

Let $Z = (V_{max} - V)/B$. The coefficient A is the slope of the regression line of the observed data $Y = (\mathrm{Log}(Z) + 1 - Z)$ with $X = t$. Practically, B can also be determined using Eq. [16], making the regression line (X, Y) pass through the origin. The corresponding value of B can then be compared with its original value calculated from the measured shrinkage curve of the sample (shrinkage cycle), using Eq. [18]. In theory, $B = K_{bs}(W_M - W_N)$, which means that B is a parameter of the S_hC. If the measured and calculated values of B are different from each other, it would be due to the fact that structure had

Table 2. Particle size, cation exchange capacity (CEC), and percentage of total CEC (S/T) for five analyzed soil samples (oxysols) of the Booro Borotou sequence in Ivory Coast (CEC and S/T come from Fritsch et al. 1989).

Sample	Clay <2 μm	Silt <20 μm	Silt <50 μm	Sand <200 μm	Sand >200 μm	CEC	S/T
	kg/(kg dry soil)					cmol kg^{-1}	%
T140	45.1	7.7	2.3	11.0	30.3	1.8	4.7
T240	49.9	5.2	3.7	11.3	29.5	2.1	30
T340	37.4	3.7	2.2	13.5	42.9	1.9	57
T440	44.7	3.1	2.2	12.0	37.1	missing	
T740	22.9	5.2	3.8	23.2	43.7	1.3	71
T840	16.6	6.3	4.4	18.1	54.4	1.1	46
T940	10.4	7.8	4.0	17.5	59.5	1.0	93

been modified between the two cycles and the hydrostructural parameters: K_{bs}, W_M and W_N are changed.

MATERIALS AND METHODS

Soil Samples

Undisturbed soil samples, 20 cm long and 10 cm high, were taken horizontally from 40- to 60-cm depth of the B horizon of seven profiles dug along a ferrallitic and ferruginous soil sequence in the Ivory-Coast. The soils were described by Fritsch et al. (1989) and correspond to Oxisols in the USDA classification. Properties of these soils are listed in Table 2.

The dry soil samples were divided into two parts; some were shaped with a knife to obtain undisturbed soil cores of 5.6 cm in diameter and 3 cm length; the others were manually disaggregated into dry fine aggregates through a 2-mm sieve.

Swelling and Shrinkage Curves of Aggregated Soil Samples

Swelling and shrinking cycles of reconstructed soil samples packed with <2-mm aggregates were performed using the apparatus and the procedure shown schematically in Fig. 4. A cell consisting of a tube, 5 cm in diameter, and 8 cm long was cemented to a rigid porous plate (250-μm pore radius) which allowed drainage or evaporation. Likewise, a freely moving porous plate was shaped to cover the sample inside the tube. A 50-g weight was placed on top of this porous plate to keep it in its horizontal position and in contact with the sample while immersed with water. A displacement sensor measured the plate movement with a resolution of >10 μm.

Each 2-mm sieved dry soil sample was packed, layer by layer, in a cell where the porous plate was placed in contact with a film of water. Each added layer was saturated with water and the sample was gently tapped on the top to remove any entrapped air. A first drying cycle was conducted where one could see samples staying coherent and shrinking in the three dimensions. A wetting and drying cycle was performed once more to ensure a good stability of the hydrostructural behavior.

The Swelling Phase

The cell containing the dry sample was placed into a beaker under the displacement transducer. The beaker was then filled with water until the water level reached the porous plate at the top of the sample (in around 20 s). This water level was maintained by successive refilling of the beaker to replace the evaporated water. Measurements of the sample height were taken every 100 s for 2 h from the start of the experiment, and every 5 min after 2 h for about 10 h (800 minutes) as shown in Fig. 4.

The Shrinkage Phase

At the end of the swelling phase, the cell was taken out of the beaker and was placed on bottling paper for approximately 1 min to drain the excess water. The cell was then placed on a balance and under the displacement sensor. Water evaporation was possible from the bottom and the top of the cell. Measurements of the weight, $M(t)$, and height of the sample, $H(t)$, were taken every 5 min until the end of the shrinkage which lasted for 8 to 10 d.

After two wetting-drying cycles, the dry soil sample was taken out of its cell and dried at 105°C and its dry weight, M_s, was measured. The specific volume and the gravimetric water content were calculated using the following equations:

$$V = V_i[H(t)/H_i]^3 \text{ and } W = [M(t) - M_s]/M_s \qquad [19]$$

where V_i and H_i are the initial specific volume and height of the sample, respectively. The pedostructural parameters were determined using the computer program CARHYS as described by Braudeau et al. (2004b).

RESULTS AND DISCUSSION

Pedostructural Parameters

Figure 5 shows a comparison between the $W_{N,M,L}$ and K_{bs} parameters of the reconstructed soil sample (y axis), obtained from the measurement of the ShC during the

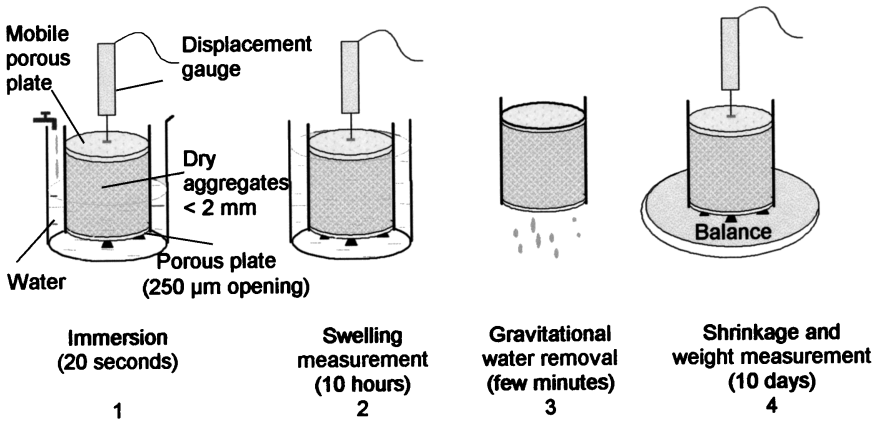

Fig. 4. Apparatus and procedure for the continuous measurements of swelling for a reconstructed soil sample immersed in water followed by shrinkage and evaporation (weight) measurements during air drying.

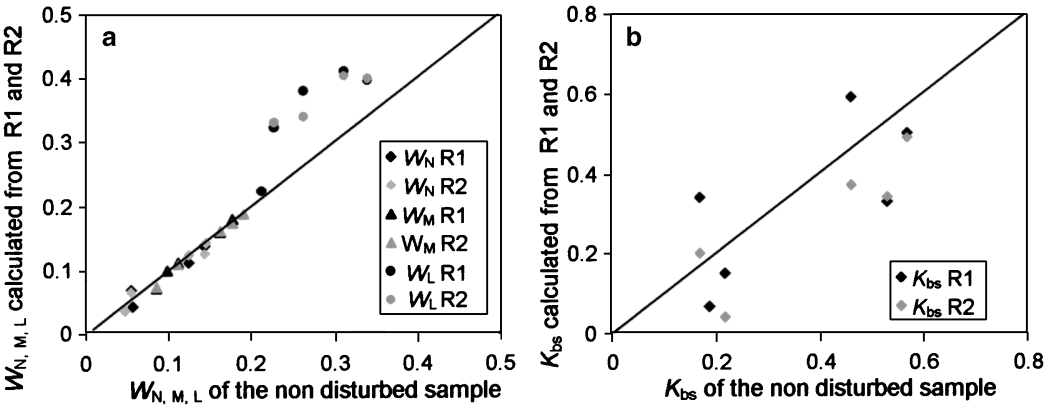

Fig. 5. Comparison between the different measurements of the structural parameters required for the swelling curve equation: a) water contents at particular points of the shrinkage curve, W_N, W_M, W_L, and b) the slope of the basic shrinkage phase K_{bs}. Parameters of the non altered soil core sample replication are put on the X-axis while on Y-axis are reported the measurements of the reconstructed aggregated soil corresponding to the shrinkage curves of the two cycles R1 and R2.

two cycles (R1 and R2), and parameters of the corresponding nondisturbed soil sample measured separately (x axis). The prefixes R1 and R2 correspond to the two shrinkage cycles of the same reconstructed aggregated soil sample. Figure 5a shows that the water content at saturation, W_L, of the disturbed soil sample is systematically superior to that of the nondisturbed control; but the parameters, W_N and W_M, which are characteristic properties of the primary peds (corresponding to the minimal and maximal pore volume of the primary peds, respectively) are quite similar for the disturbed and nondisturbed soils. That means that the soil preparation procedure changed the interaggregates porosity but did not change the functionality of the primary peds. However, we can observe in Fig. 5b that the relationship between the primary peds level and the assembly, represented by K_{bs} (Eq. [2]), was different in the two cycles. It was also different for the disturbed and not disturbed soil samples. That means that the structure of the reconstituted soil cores was fragile and not very stable, certainly because of their preparation: they were not compacted enough so their specific volumes were much greater than those of the natural samples.

Swelling and Shrinkage Curves of Soil Aggregates

The two cycles of swelling-shrinkage of the soil sample T140 are given as an example in Fig. 6. Because of

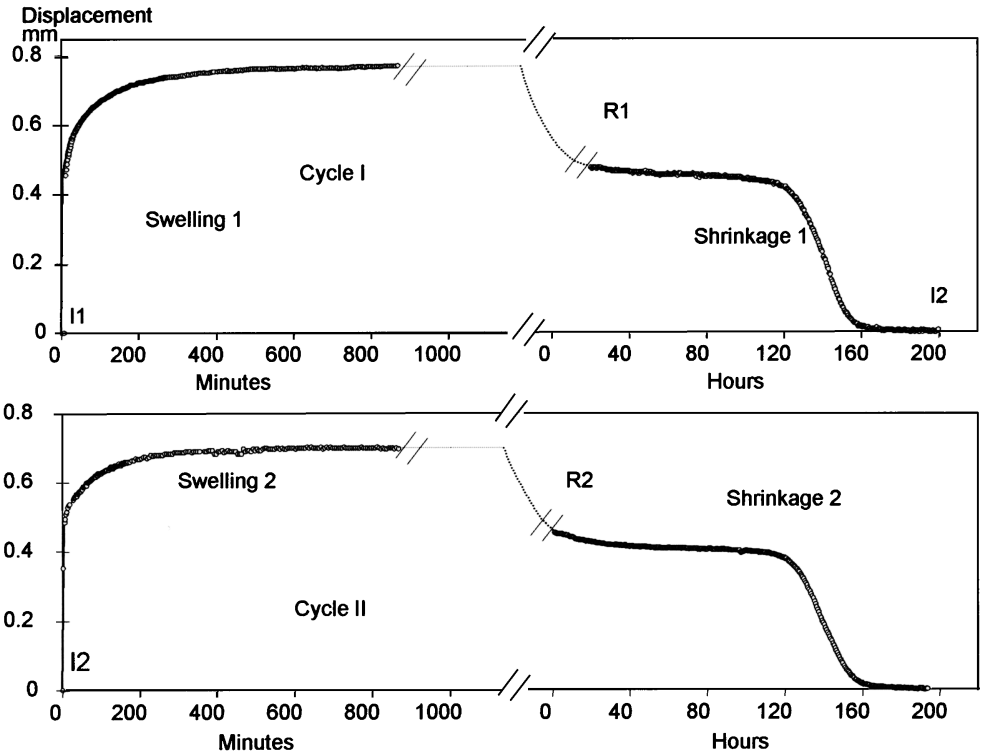

Fig. 6. Sample results of continuous measurements of two swelling-shrinkage cycles for T140 soil.

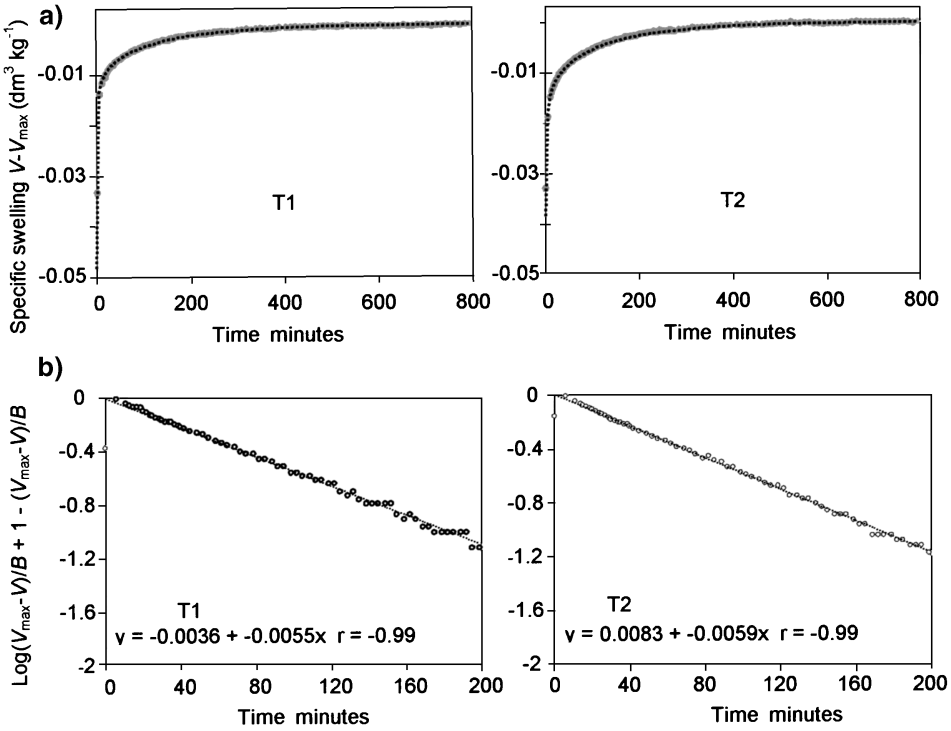

Fig. 7. a) Swelling curves of two successive swelling-shrinking cycles of the T140 soil sample; dark dots represent the modeled swelling curve and the gray circles are the measured data. b) The corresponding linear regression according to Eq. [16] to determine the coefficient $A = \rho_w k_{mi} E_{mi}/(W_M - W_N)^2$; circles are the measured data.

the high resolution of the change in height measurement (10 μm), it was assumed that the height of the soil sample in the dry state was exactly the same in each cycle. So it was taken as the origin of the *y*-axis.

The difference in the sample height at the end of the swelling and the beginning of shrinkage was due to the interpedal shrinkage occurring during drainage on the bottling paper, which was not measured. I1 and I2 in Fig. 6 represent the immersion of the soil sample in the first and second cycle, and R1 and R2, the nonmeasured interpedal shrinkage. Figures 5 and 6 show good reproducibility of the two cycles. Total shrinkage varied only slightly between the first and the second cycle. This variation is correlated to K_{bs} and reflects a slight change of aggregate arrangement during the two cycles for this sample.

For all the tested soils, we found an excellent linear correlation (Fig. 7) between time of swelling and the left term of Eq. [16]. The coefficient of determination was higher than 0.99 (Table 3). The sum of squared deviations between the calculated curve $t = f(V_{max} - V)$ (Eq. [16]) and the observed data was about 10^{-8}. One can note in Fig. 7 that the two curves are practically superimposed. The parameters A, B, V_{max} and the product $[K_{bs}\ \max(w_{bs})]$ are listed in Table 3. For certain samples, B and the product $[K_{bs}\ \max(w_{bs})]$ are quite different. This difference is attributed to K_{bs} rather than $\max(w_{bs})$, which is a characteristic of the primary peds and more stable than the latter (Fig. 5). In addition, K_{bs} is a structural parameter defined by Eq. [2] and was calculated from experimental data assuming an isotropic volume change. Therefore, K_{bs} may be over or underestimated, depending on the real degree of anisotropy of the shrinkage process.

Table 3. Values of the swelling curve characteristic parameters obtained by linear regression of soil aggregates swelling data.

Sample	V_{max}	$K_{bs}(W_M - W_N)$	B	A	$t_{1/2}$ s	R^2†	SSD‡
	$dm^3 kg^{-1}$	$dm^3 kg^{-1}$	$dm^3 kg^{-1}$	$10^{-5} s^{-1}$			10^{-6}
T140	0.785	0.017	0.016	9.195	2100	0.998	0.017
T240	0.789	0.025	0.02	9.753	1980	0.998	0.023
T340	0.758	0.025	0.014	9.195	2100	0.998	0.021
T440	0.761	0.022	0.012	7.850	2460	0.988	0.04
T740	0.662	0.015	0.011	8.940	2160	0.998	0.004
T840	0.602	0.004	0.009	0.292	660	0.985	0.033
T940	0.605	0.005	0.009	0.214	900	0.990	0.012

† Coefficient of determination.
‡ Sum of squared deviations.

Accordingly, Eq. [14] to [16] represents the kinetics of absorption of water by swelling of the primary peds. They can be expressed in a standardized form as:

$$(1 - z)\exp(z) = \exp(-At) \qquad [20]$$

where z is a measure of the degree of swelling which, according to Eq. [2] to [5] and neglecting the role of W_{ma} in the swelling process, can be computed using:

$$z = (V - V_{min})/(V_{max} - V_{min});\ z = w_{bs}/w_{bs\,max};$$
$$z = (Vp_{mi} - Vp_{mi-min})/(Vp_{mi-max} - Vp_{mi-min});\ \text{or}$$
$$z = (H - H_{min})/(H_{max} - H_{min});$$

H being the height of the soil core sample.

From Eq. [20], the time to half swelling, $t_{1/2}$, is calculated for $z = 0.5$ as:

$$t_{1/2} = -[\mathrm{Ln}(0.5) + 0.5]/A = 0.1931/A \qquad [21]$$

Table 4. Values of E_{mi} and k_{mi} calculated according to Eq. [7] and [17], and the assumption made on the relationship between h_{ma}, Ps_{mi} and Pc in Fig. 3. Parameters of the tensiometric curve, Ema, σ, and $h°_{ma}$ come from Braudeau and Mohtar (2004).

Sample	E_{ma}	σ	$h°_{ma}$	E_{mi}	Junction†	$k_{mi} \times 10^8$
	Jkg^{-1}	$kgkg^{-1}$	kPa	Jkg^{-1}	kPa	$kg_w\ kg^{-1}_s\ kPa^{-1}s^{-1}$
T140	1.16	0.012	8.6	2.1	72	8.47
T240	1.40	0.007	11.5	2.0	71	9.44
T340	1.07	0.013	11.7	1.7	61	7.40
T740	1.06	0.010	9.9	2.6	70	6.35
T940	0.93	0.012	6.1	2.4	62	1.29

† Point for which $Ps_{mi} = h_{ma}$ in Fig. 3.

and can be used instead of A for the parameter in the swelling curve Eq. [20].

It is remarkable that the values of $t_{1/2}$ listed in Table 3 are quite constant for the first five samples despite the changes in their clay content (Table 2). However, the difference between these first values, near 2100 s, and those (660 and 900 s) of the last two samples, confirms the difference in behavior observed by Braudeau and Bruand (1993) between the red kaolinitic soils at the upper part of the sequence, and the hydromorphic ferruginous soils at the lower part of the sequence. This difference is explained by the change in mineralogy related to the apparition of smectite in the latter (Fritsch et al., 1989).

Micropore Swelling Pressure (Ps_{mi}) and Exchange Rate Coefficient (k_{mi})

The swelling kinetics given by Eq. [16] is based on Eq. [7], which relates the swelling pressure Ps_{mi} to the independent state variable, w_{bs}. The good fit between measured and calculated swelling curves supports the validity of Eq. [7] of Ps_{mi} and the good choice of the variable (w_{bs}). The product $k_{mi}E_{mi}$ in Eq. [17] can be determined from experimental data using the regression (X,Y) and knowing W_N and W_M. If the assumptions made for the graph of Ps_{mi} and Pc in Fig. 3 are valid, E_{mi} is then determined by the tensiometric curve. That allows calculating the exchange rate coefficient, k_{mi}, using Eq. [17] in ($kg_{water}\ kg^{-1}{}_{solids}\ kPa^{-1}\ s^{-1}$). For the soils studied here, E_{mi} and k_{mi} were calculated using the tensiometric curves presented in Braudeau and Mohtar (2004) and are given in Table 4. We note that the resulting curve in Fig. 3, which is the portion of h_{ma} curve from saturation up to the point of junction with the Ps_{mi} curve, can be considered as the suction curve $h(W)$ for the range of W, from saturation to the air entry point in primary peds, W_B (with $W_B > W_N$).

CONCLUSIONS

This paper presents a model for the swelling rate of a dry aggregated soil sample immersed in water. The developed equations use the pedostructure variables and parameters defined from the shrinkage curve. We established the swelling curve equation for a dry bed of packed aggregates immersed in water, which is principally based on an expression of the swelling pressure in primary peds that was adapted from the Voronin (1980) Eq. [6] to the pedostructure characteristics. Accordingly, new notions were defined such as the swelling (hydration) pressure of primary peds, micro, and macro suction pressures, equilibrium between micro and macro pore water pools, and micro-macro pore water exchange rate. The modeled swelling curve compared very well with the measured data, which corroborates these new notions. Methods for calculating and estimating the characteristic parameters of the different equations, including the swelling pressure, are presented and discussed.

ACKNOWLEDGMENTS

The authors thank the support of the Chicago French Consulate Science attaché's office and the Organization for Economic Cooperation and Development (OECD). Part of this work was completed while the two authors were hosted by the Civil Engineering Department at the American University of Beirut. Special thanks to Professor Mounir Mabsout and Ms Zakia Deeb and the rest of Civil Engineering team at AUB for their support.

REFERENCES

Berezin, P.N., A.D. Voronin, and Y.V. Shein. 1983. An energetic approach to the quantitative evaluation of soil structure. Pochvovedeniye. 10:63–69.

Braudeau, E., and A. Bruand. 1993. Détermination de la courbe de retrait de la phase argileuse à partir de la courbe de retrait établie sur échantillon de sol non remanié. Application à une séquence de sol de Côte-d'Ivoire. C.R. Acad. Sci. Paris. 307:685–692.

Braudeau, E., and R.H. Mohtar. 2004. Water potential in nonrigid unsaturated soil-water medium. Water Resour. Res. 40:W05108.

Braudeau, E., R.H. Mohtar, and N. Chahinian. 2004a. Estimating soil shrinkage parameters. p. 225–240. *In* Y. Pachepsky and W. Rawls (ed.) Development of pedotransfer functions in soil hydrology, Elsevier, Amsterdam.

Braudeau, E., J.P. Frangi, and R.H. Mothar. 2004b. Characterizing nonrigid dual porosity structured soil medium using its Shrinkage Curve. Soil Sci. Soc. Am. J. 68:359–370.

Bronswijk, J. 1988. Modelling of water balance cracking and subsidence in clay soils. J. Hydrol. (Amsterdam) 97:199–212.

Chertkov, V.Y. 2004. A physically-based model for the water retention curve of clay pastes. J. Hydrol. (Amsterdam) 286:203–226.

Favre, F., P. Boivin, and M. Woperesis. 1997. Water movement and soil swelling in a dry cracked Vertisol. Geoderma 78:113–123.

Fritsch, E., A.J. Herbillon, E. Jeanroy, P. Pillon, and O. Barres. 1989. Variation minéralogiques et structurales accompagnant le passage « sols rouges-sols jaunes » dans un bassin versant caractéristique de la zone de contact forêt-savane de l'Afrique occidentale (Booro Borotou, Côte d'ivoire). Sci. Géol. Bull. 42:65–89.

Greco, R. 2002. Preferential flow in macroporous swelling soil with internal catchment: Model development and applications. J. Hydrol. (Amsterdam) 269:150–168.

Hammel, K., J. Gross, G. Wessolek, and K. Roth. 1999. Two-dimensional simulation of bromide transport in a heterogeneous field soil with transient unsaturated flow. Eur. J. Soil Sci. 50:633–647.

Horn, R., T. Way, and J. Rostek. 2003. Effect of repeated tractor wheeling on stress/strain properties and consequences on physical properties in structured arable soils. Soil Tillage Res. 73:101–106.

Kim, D., R. Angulo-Jaramillo, M. Vauclin, Y.Y. Feyen, and S. Choi. 1999. Modeling of soil deformation and water flow in a swelling soil. Geoderma 92:217–238.

Kim, D., F. Diels, and J. Feyen. 1992. Water movement associated with overburden potential in a shrinking marine clay soil. J. Hydrol. (Amsterdam) 133:179–200.

Kirby, J., and A. Ringrose-Voase. 2000. Drying of some Philippine and Indonesian puddled rice soils following surface drainage: Numerical analysis using a swelling soil flow model. Soil Tillage Res. 57: 13–30.

Logsdon, S.D. 2002. Determination of preferential flow model parameters. Soil Sci. Soc. Am. J. 66:1095–1103.
Low, P.F. 1987. Structural component of the swelling pressure of clays. Langmuir 3:18–25.
Michel, J.C., A. Beaumont, and D. Tessier. 2000. A laboratory method for measuring the isotropic character of soil swelling. Eur. Soil. Sci. 51:689–697.
Rollins, M., M. Hallam, and V. Myers. 1961. The apparent swelling behaviour of some moderately dispersed bentonites. Soil Sci. Soc. Am. Proc. 25:407–409.
Ruy, S., L. Di Pietro, and Y.M. Cabidoche. 1999. Numerical modelling of water infiltration into the three components of porosity of a vertisol from Guadeloupe. J. Hydrol. (Amsterdam) 221:1–19.
Sarmah, A., U. Pillai-McGarry, and D. McGarry. 1996. Repair of the structure of a compacted Vertisol via wet/dry cycles. Soil Tillage Res. 38:17–33.
Van Dam, J.C. 2000. Simulation of field-scale water flow and bromide transport in a cracked clay soil. Hydrol. Processes 14:1101–1117.
Voronin, A.D. 1980. The structure-energy conception of the hydrophysical properties of soils and its practical applications. Pochvovedeniye. 12:35–46.
Wells, R., D. Di Carlo, T. Steenhuis, J.Y. Parlange, M. Römkens, and S. Prasad. 2003. Infiltration and surface geometry features of a swelling soil following successive simulated rainstorms. Soil Sci. Soc. Am. J. 67:1344–1351.